Atmos. Chem. Phys. Discuss., 11, 7811–7849, 2011
www.atmos-chem-phys-discuss.net/11/7811/2011/
doi:10.5194/acpd-11-7811-2011

Atmospheric Chemistry and Physics Discussions

Improvement of ozone forecast over Beijing based on ensemble Kalman filter with simultaneous adjustment of initial conditions and emissions

X. Tang, J. Zhu, Z. F. Wang, and A. Gbaguidi

LAPC and ICCES, Institute of Atmospheric Physics, Chinese Academy of Sciences, Beijing, China

Received: 18 February 2011 – Accepted: 1 March 2011 – Published: 8 March 2011

Correspondence to: J. Zhu (jzhu@mail.iap.ac.cn)

Published by Copernicus Publications on behalf of the European Geosciences Union.

Abstract

We performed ozone data assimilation by simultaneously adjusting the ozone initial conditions, precursor initial conditions and emissions based on the Ensemble Kalman Filter (EnKF) and assessed its impacts on ozone modeling and forecasting in Beijing and nearby regions. A high-resolution regional air quality model and a newly established regional monitoring network covering Beijing and its surrounding areas were employed. At each assimilation cycle, the forecast error covariance was sampled from a set of forecast ensembles that were generated by perturbing ozone precursor initial conditions, emissions, photolysis rates and deposition velocity. A model-error module and a local analysis scheme have been introduced to reduce the impact of filter divergence and spurious correlation that accompanied with EnKF. The results showed significant improvement of 1-hour ozone forecast in Beijing and its surrounding areas through separately adjusting ozone initial conditions, precursor initial conditions and emissions with ozone observations. However, adjustment of precursor initial conditions and emissions had minor effect on the 1-hour ozone forecast in suburban area. The best ozone forecast skill was obtained through jointly adjusting ozone initial conditions, NO_x and VOC initial conditions and emissions. The root mean square errors of 1-hour ozone forecast at urban sites and suburban sites decreased by 54% and 59% respectively compared with those in free run. Furthermore, the specific impacts of observations from urban and suburban sites on ozone data assimilation were evaluated by implementing sensitivity experiments. Both urban and suburban sites were found to be very important for the improvement of regional ozone forecast. The importance of observational data at urban sites was particularly highlighted through its role in constraining the uncertainty of precursor initial conditions and emission rates. Further improvement of regional ozone forecast might therefore be expected with more routine regional air pollution monitoring stations.

1 Introduction

As one of the typical city clusters in China, Beijing and its surrounding areas are facing serious challenge of regional air pollution. Among all the regional air pollution problems, high surface ozone is one of the most serious problems, which is also one of the key issues in the CAREBeijing campaign. It is not only an important pollutants but also closely related to the formation of other important pollutants such $PM_{2.5}$ and PM_{10}. The daily maximum ozone concentration of urban Beijing in summer has increased from 80 $\mu g\,m^{-3}$ in 1982 to 250 $\mu g\,m^{-3}$ in 2003 (Shao et al., 2006), much higher than whole China's air quality class-II standard (160 $\mu g\,m^{-3}$ for hourly ozone). Ozone is powerful respiratory irritant; it can reduce the body's resistance to infection. Exposure to high levels of ozone may lead to large reduction in lung function, inflammation of the lung tinning and more frequent and severe respiratory diseases. Therefore, providing ozone forecast in Beijing is undoubtedly as important as PM_{10} prediction, not only for an effective control strategy, but also for public. On the other hand, forecasting and early warning of ozone pollution is needed during Beijing Olympic Games in order to ensure a health environment for athletes and attendees. However, large uncertainty still exists in the current numerical ozone forecasting and modeling in Beijing and neighboring regions. Around 30 ppbv of root mean square error was reported for ozone forecast in Beijing during the 2008 Olympic Summer Games with the Nested Air Quality Prediction Model System (Tang et al., 2010a). This study attempts to reduce the uncertainty of ozone forecast at Beijing and its surrounding areas by assimilating ozone observational data into a regional air quality modeling system. The newly established regional air quality observation network covering Beijing, Tianjin and Hebei Province now provides valuable information on spatial and temporal variations of ozone.

Data assimilation is a data analysis technique which integrates observational information into three-dimensional model to obtain better estimation of state variables or parameters. Several applications of data assimilation method in ozone modeling brought out relevant findings for ozone forecast improvement in many locations (Chai

Discussion Paper | Discussion Paper | Discussion Paper | Discussion Paper |

ACPD

11, 7811–7849, 2011

Improvement of ozone forecast over Beijing

J. Zhu et al.

et al., 2006; Elbern et al., 2007; van Loon et al., 2000; Hanea et al., 2004; Constantinescu et al., 2007). However, data assimilation for ozone forecast over Beijing region was weakly documented.

The difficulties in ozone forecast of Beijing and its surrounding areas to a large extent lie in the complex processes of surface fluxes, flow, turbulent transport and chemical reactions that control ozone concentrations. Previously, many studies have identified some important factors including photolysis frequencies (Li et al., 2011), regional transport (Streets et al., 2007; Wu et al., 2011) and ozone initial conditions (Tang et al., 2010b). On the other hand, rapid and complex perturbations of air pollutant emission rates occur in these areas, with significant uncertainties of NO_x and VOC emissions, which are two of the most important ozone precursors. For instance, the number of motor vehicles in Beijing rocketed from about 3.5 million in 2008 to around 5 million in 2010. At the same time, however, several emission reduction measures such as traffic restriction are conducted. These changes can hardly be described only with the existing emission inventory updated once for 2–3 years, inducing large uncertainty into ozone modeling. Therefore, an efficient way to control the errors in ozone forecast is needed to reduce the errors in ozone initial conditions, precursor initial conditions and emissions, at least from a regional perspective. For this purpose, we employed the ensemble Kalman filter (EnKF) method associated with the regional observational network. In order to obtain the most effective assimilation on ozone forecast, we experienced several strategies including separated and simultaneous adjustments of ozone and precursor initial conditions and emissions with a compared analysis of the impacts of urban and suburban sites on the data assimilation performance.

Section 2 describes the methodology adopted in this study, results and discussions are presented in Sect. 3, and conclusions are given in Sect. 4.

ACPD
11, 7811–7849, 2011

2 Methodology

2.1 Data assimilation with EnKF

EnKF, introduced by Evensen (1994), is an approximate version or extension of Kalman filter. It employs Monte Carlo approach to represent the uncertainty of variable with a large stochastic ensemble. In this way, the uncertainty can evolve nonlinearly with ensemble forecast, and flow-dependent background error covariance can be obtained from the forecast ensemble results. Thus, the measurements can be integrated into model in a physical consistent way. Compared with the four-dimensional variation, another advanced data assimilation approach, it does not require an adjoint model and is easy to implement. A detailed introduction of the EnKF theory and its applications for atmospheric and ocean researches are provided by Evensen (2009).

An EnKF data assimilation system has been developed for dust storm forecast over China and brings significant improvement of forecast skill (Lin et al., 2008a, b; Zhu et al., 2009). The dust storm forecast is mainly dependent on emission and transport without considering chemical reaction. In this study, the EnKF data assimilation system is used for the ozone forecast which includes not only processes of emissions and transport but also the complex chemical reactions. The system is employed for constraining input uncertainties of ozone modeling including ozone initial conditions, precursor (NO_x, VOC) initial conditions and emissions. The implementation of EnKF and its detailed setup are as following.

Initial perturbation of control variables

The forecast process of state variable in a chemical transport model can be simply represented by:

$$x_{t+1} = \mathrm{M}(x_t, p_{i=1,n}) \tag{1}$$

Discussion Paper | Discussion Paper | Discussion Paper | Discussion Paper |

ACPD

11, 7811–7849, 2011

Improvement of ozone forecast over Beijing

J. Zhu et al.

where x_{t+1} represents the forecast state variable at the time step $t+1$, and M denotes the model operator. $p_{i=1,n}$ represents the model inputs of precursor initial conditions and emission rates. The uncertainty in the first guess value of x_t and $p_{i=1,n}$ can evolve with model integration and are induced into the forecast results. A key process of EnKF is using a group of stochastic ensemble samples to represent the uncertainty of control variables (ozone initial conditions, precursor (NO_x, VOC) initial conditions and emission rates)

$$V_t = \begin{bmatrix} x_t+\varepsilon_1, x_t+\varepsilon_2, \ldots, x_t+\varepsilon_N \\ p_i+\gamma_1, p_i+\gamma_2, \ldots, p_i+\gamma_N \\ \ldots \end{bmatrix} = \begin{bmatrix} X_t \\ P_t \end{bmatrix} \tag{2}$$

X_t represents the ensemble of ozone. P_t denotes the ensemble of precursor initial values and emission rates. N is the ensemble size set as 50, which have been proved to be credible by previous publications (Carmichael et al., 2008; Constantinescu et al., 2007). ε and γ represent random initial perturbation samples which are added to first guess value of control variables at initial time.

Ideally, initial perturbations should reflect the characterization of initial errors of first guess value (Evensen, 2003). Different from the great impact of initial perturbation on meteorological and ocean data assimilation, initial perturbation of state variables in chemical transport model has a relatively small influence on performance of EnKF. Promised results of ozone data assimilation with EnKF have been obtained by Wu et al. (2008) in which initial perturbation is not applied. In the present study, the strategy which has been proven credible by Evensen (1994) is employed to generate initial perturbation fields for its simplicity in implementation. The spatial correlation scale of initial perturbation fields are set as 54 km in horizontal and 3 model grids in vertical after several sensitivity tests. The perturbations are assumed to be within 50% of the first guess values for initial conditions of $O_{3,}$ NO_x and VOC. Perturbation ranges of NO_x and VOC emission rates are set as 60% and 80% of based emission rates according to the uncertainty analysis results of Tang et al. (2010b). Since the correlations

Discussion Paper | Discussion Paper | Discussion Paper | Discussion Paper |

ACPD

11, 7811–7849, 2011

Improvement of ozone forecast over Beijing

J. Zhu et al.

between control variables are hard to obtain directly, they are assumed to be independent with each other for initial perturbation. These correlations between state variables and emissions can be reconstructed with model integration. It should be noteworthy that the correlations between the two emissions cannot be reconstructed with model integration. It may lead to underestimation of the correlation between them and affect background error covariance. This issue is beyond the scope of this paper and further investigations are needed.

Forecast and update of control variables

The second step of EnKF is using the initial samples of control variables as inputs to implement several simulations with the original model operator. The prediction of control variables with ensemble simulation can be represented by $V_{t+1}^f = MV_t$. The background error covariance is calculated by:

$$B_{t+1}^f = \frac{(V_{t+1}^f - \bar{V}_{t+1}^f)(V_{t+1}^f - \bar{V}_{t+1}^f)^T}{N-1} \tag{3}$$

where $\bar{V}_{t+1}^f$ is the ensemble mean of V_{t+1}^f. The observed values of state variables are also assumed to be uncertain, and an ensemble of observation values $Y_{t+1} = [y_{t+1} + \tau_1, y_{t+1} + \tau_2, \ldots, y_{t+1} + \tau_N]$ is obtained by adding random perturbations $\tau$to the observed values $y_{t+1.}$ The observation error covariance is calculated by:

$$R_{t+1} = \frac{(Y_{t+1} - \bar{Y}_{t+1})(Y_{t+1} - \bar{Y}_{t+1})^T}{N-1} \tag{4}$$

The observation errors, including both representative error and measurement error, are assumed to be uncorrelated in time and space. The perturbations for observation are within 10% of the observed ozone concentration as suggested by von Loon et al. (2000).

ACPD
11, 7811–7849, 2011

Based on the error statistics of simulation and observation, the simulated values of control variables in three-dimensional space and surface observations are combined to update the estimation of control variables:

$$V_{t+1}^{a} = V_{t+1}^{f} + K(Y_{t+1} - HV_{t+1}^{f}) \tag{5}$$

$$K = \frac{B_{t+1}^{f} H^{T}}{(HB_{t+1}^{f} H^{T} + R_{t+1})} \tag{6}$$

H is the projection operator to interpolate the simulated values in three-dimensional model space into these in observational space. K is the Kalman gain which is calculated based on the background and observation error covariance. It projects the departure between simulation and observation in observational space ($Y_{t+1} - HV_{t+1}^{f}$) to increment of control variables in model space. The ozone observations of different sites are integrated into model in a sequential way. At every update step only observation of one site is assimilated, and then the updated field of control variables is used as the background for assimilating observation of next site. The sequential way is suggested to be better than the way with observations of all sites assimilated at the same time (Houtekamer and Mitchell, 2001).

Assimilation with localization and model error

A major problem in EnKF is the spurious correlation between the ensembles of two independent variables. It is caused by using finite ensemble size and can result in spurious update of control variables and underestimation of analysis error covariance. A local analysis scheme is employed in this study to reduce the impact of spurious correlation between the ensembles of two grids which are far away from each other. Only observations within a certain distance (localization scale) from the analysis grid are used for updating the control variable in this grid. An optimal localization scale can

ACPD
11, 7811–7849, 2011

efficiently remove the influence of spurious correlation, while not degrading the effect of observation. The optimal localization scale can vary with ensemble size, dynamic system and life cycle of chemical species. In this study, 54 km of localization scale is set for updating ozone initial conditions and 45 km for updating precursor initial conditions and emissions after several sensitivity tests.

Another problem in EnKF is filter divergence which are shown by underestimation of the weight of observation and even disregarding of observation during update of control variable. A simple method to prevent filter divergence is inflating background error covariance before or after updating control variable (Constantinescu et al., 2007). The main drawback of inflation method is lack of physical or chemical constraint. Therefore, it can lead to spurious linear increase of background error covariance at the area far away from observation sites. The dynamic and chemical balance of model may be destroyed by the inflation. In this study, however, we employ another approach to reduce the impact of filter divergence without destroying the model balance.

In fact, besides the spurious correlation induced by finite ensemble size and its resulting underestimation of analysis error covariance, another important reason for filter divergence is the neglect of model errors. For chemical transport model, the errors from surface parameters such as emissions and deposition are quit important for estimating background error covariance. Tang et al. (2010b) have identified the major uncertainty sources of regional ozone forecast in Beijing and its surround areas which includes precursor emissions, photolysis rate and dry deposition velocity. Therefore, we integrate these important errors into the forecast ensembles of EnKF through perturbing these factors. With reference to the uncertainty analysis of Tang et al. (2010b), the perturbation ranges are set as 60%, 80%, 30% and 25% of their first guess values for NO_x and VOC emission rates, photolysis rate of NO_2 and dry deposition velocity respectively. The evolvement of these errors in time is simulated by a first order linear Markov model:

$$q_{t+1} = \alpha q_t + \sqrt{1-\alpha^2} w_t \tag{7}$$

where q_t represents the error at the time step t. w_t is random white noise added at each time step. α is the decorrelation length of errors in time, set as 24 h. Similar model can be found in the study of Evensen (2003).

2.2 Regional air quality model

The chemical transport model used with EnKF is the Nested Air Quality Prediction Modeling System (NAQPMS). NAQPMS has been applied to simulating chemical process and transport of ozone (Li et al., 2009; Tang et al., 2010c), modeling process of aerosol and acid rain (Li et al., 2011; Wang et al., 2002) and providing operational air quality forecast in mega cities such as Beijing and Shanghai (Wang et al., 2006b). As a multi-scale air quality model NAQPMS can provide forecast of both primary and secondary pollutant from regional to urban scale. It includes modules of emissions, diffusion, advection/convection, deposition and gas/aqueous chemistry. The process of gas phase chemistry is modeled with the Carbon-Bond Mechanism Z (CBM-Z) proposed by Zaveri and Peters (1999). A revised version of RADM aqueous-phase chemistry (Wang et al., 2002) is served to simulate the aqueous-phase chemistry. The dry deposition modeling follows the scheme of Wesely (1989). The hourly meteorological driver of chemical transport model is provided by the Fifth-Generation NCAR/Penn State Mesoscale Model (MM5) (Grell, 1994) and the initial and boundary conditions of MM5 is obtained from NCAR/NCEP $1^{\circ} \times 1^{\circ}$ reanalysis data. The outputs of a global transport model CHASER (Sudo et al., 2002) at three hour intervals are used to provide the initial and boundary conditions of chemical transport model. Vertically, twenty layers with terrain following coordinates are configured with the height of the top-layer 15 km and that of the first layer near the surface 50 m. A more detailed description of this model can be found in previous publications (Li et al., 2007; Wang et al., 2006a).

The simulation in this study is configured with three nested model domains (displayed in Fig. 1a). The focus is on the third domain, covering Beijing and its surrounding areas. The gridded emission data of the three domains is prepared as following. Firstly, the INTEX-B Asia inventory for 2006 with a 0.5° resolution (Zhang et al., 2009)

ACPD
11, 7811–7849, 2011

is served as the regional emission inventory for all model domains. Then the power emissions of Beijing and its surrounding provinces (Tianjin, Hebei, Shanxi, Inner Mongolia and Shandong) in INTEX-B emission are replaced by the power plant emission dataset with exact longitude and latitude of point sources (Hao et al., 2007). The other emissions of Beijing in INTEX-B emission are also updated with the industrial boiler, domestic, industrial process emissions, and with the mobile emissions derived from Mobile 6 in SMOKE according to the traffic flow from the annual report of Beijing Traffic Development Research Center in 2006. Furthermore, the emission reductions conducted in Beijing and its surrounding areas for the 29th Olympic Games is forced into the above emission inventory according to the "29th Olympic Games Beijing air quality protection measures", which is developed jointly by the governments of Beijing, Tianjin, Hebei, Shanxi, Inner Mongolia and Shandong. Previous publications provide more details for the emission control measures during the Beijing 2008 Olympic Games (Wang et al., 2009). Finally, the emission inventory prepared above is transformed to three-dimensional gridded emissions through the Sparse Matrix Operator Kernel Emissions (SMOKE) model (Houyoux et al., 2000).

3 Regional air quality observation network

The regional air quality observational network employed in this study covers Beijing, Tianjin and Hebei province and was established in 2008 as part of the 29th Olympic Games Beijing air quality prediction. The main purpose of this network is to assess the regional air quality and the impact of regional pollutant transport on air quality of Beijing. This network is an integrated multi-dimensional monitoring network with tower, laser and surface monitoring devices etc. Hourly observed atmospheric pollutant concentration, including O_3, NO_x, SO_2, CO, $PM_{2.5}$, are provided by this network in real-time way during 1 July 2008 to 20 September 2008. It has been used to analyze the characterization of air quality in Beijing and its surrounding areas during the Beijing 2008 Olympic Games (Xin et al., 2010). Furthermore, it has been employed to evaluate model performance (Zou et al., 2010) and to improve forecast skill of an ozone ensemble forecast system (Tang et al., 2010a). This study is the first attempt to use this regional air quality network for data assimilation. Figure 1b displays the distribution of the seventeen monitoring stations in this network. There are six urban sites at the surrounding cities of Beijing (Baoding, Cangzhou, Qinghuangdao, Shijiazhuang, Tangshan, Tianjin), five urban sites at Beijing (Changping, Beida, Beiyi, IAP, Yangfang,) and six suburban sites close to Beijing (Langfang, Xianghe, Xinglong, Yanjiao, Yufa, Yongledian). The urban sites are located at the central urban area with high emission rates, while the suburban sites are located away from the central urban area with a relatively low emission rate.

3.1 Experiment design

The experiments designed are shown in Table 1. Firstly, a free run of model (EXP0) is conducted without data assimilation. It is taken as a reference for evaluating the performances of the data assimilation experiments. EXP1 is designed to investigate the effects of optimizing ozone initial value on ozone forecast with the current regional air quality network. EXP2 and EXP4 are designed to test the cross-species data assimilation strategy in which NO_x and VOC initial conditions are adjusted respectively with assimilating ozone observations. EXP3 and EXP5 are conducted to provide insight into the benefits and shortcomings with adjusting the precursor emission rates when ozone observations are used only. A simultaneous adjustment of both ozone initial conditions and precursor (NO_x and VOC) initial conditions and emission with ozone observations is also implemented in EXP6. In order to evaluate the roles of observations from urban sites and suburban sites in ozone data assimilation, two sensitivity experiments are carried out with only observations of urban sites assimilated in EXP6u and those of suburban sites assimilated in EXP6s. In order to independently evaluate the performance of data assimilation, ozone observations at two urban sites (IAP and Yangfang) and one suburban site (Langfang) are withdrawn from assimilation for all the experiments.

Discussion Paper | Discussion Paper | Discussion Paper | Discussion Paper |

ACPD

11, 7811–7849, 2011

In all the experiments, we firstly conducted two-week spin-up simulation without perturbation to reduce influences of initial conditions. Then initial perturbations were added to the initial conditions of control variables at 19:00 on 12 August 2008 (LT), while ensemble simulations started at the same time. In order to ensure the balance of model state after perturbation and obtain flow-dependent background error covariance for EnKF, five hour spin-up ensemble simulations are conducted. At 00:00 on 13 August 2008 (LT) the observed data of surface ozone start to be assimilated hour by hour. The assimilation ended at 23:00 on 13 August 2008 (LT). In addition, evaluation focuses on the performance of 1-hour ozone forecast after assimilating observational data. Although the 1-hour short term ozone forecast may not as valuable as much longer forecast such as 24-hour or 48-hour forecast in application, it can provide quick responses of ozone forecast after assimilating observation and identify advantages and disadvantages of different assimilation strategies.

4 Results and discussion

4.1 Adjustment of ozone initial conditions

We first look at the results from EXP1, in which only the ozone initial conditions are adjusted by assimilating ozone observations. Figure 2a and b present a comparison of observed daytime ozone values of the monitoring stations against simulated daytime ozone concentrations in free run (EXP0) and EXP1 respectively. In the free run, high ozone concentrations can be observed at Tianjin and Beijing with the maximum values over 80 ppbv, as well as the downwind areas of Beijing with the maximum values over 60 ppbv. It is obvious that ozone concentrations are overestimated by model in the urban areas of Beijing, Tianjin and the suburban areas between them but underestimated in the urban areas of Tangshan. After optimizing ozone initial conditions in EXP1, the overestimation is weakened to a large extent for the 1-hour ozone forecast, especially at the urban and suburban areas of Beijing with abundant monitoring stations. It should be noted that the simulated ozone concentrations are also much lower than those of free run at the downwind areas of Beijing where no monitoring station available. This modification at downwind areas probably originates from the optimization of ozone initial conditions at upwind areas such as Beijing. It indicates that adjusting ozone initial conditions with EnKF not only optimize ozone simulation in the areas with abundant observations, but also provides potentials of improving those in the areas with no observations and obtaining better estimation of regional ozone transport.

As shown in Fig. 3, a comparison is made between the root mean square error (RMSE) of 1-hour ozone forecast at individual sites in free run and those in EXP1. Significant improvement of ozone forecast skill can be claimed after adjustment of ozone initial conditions. The RMSE averaged over urban sites is reduced by 38% and that over suburban sites reduced by 57%. The sharp decrease of RMSE at suburban sites indicates that the uncertainty of ozone initial value plays a very important role for short term ozone forecast in suburban area. A relatively smaller decrease of RMSE at urban sites than that at suburban sites is probably caused by the quite complex uncertainty sources for ozone forecast in the urban areas. In order to further understand the different effects of adjusting ozone initial conditions on ozone forecast at urban and suburban sites, the hourly ozone concentrations from observations, model free run, analysis and 1-hour forecast in EXP1 at two urban sites and two suburban sites are displayed in Fig. 4.

Obvious overestimation of ozone concentration is observed at the two suburban sites (Yanjiao and Yufa) in the free run. After the strong adjustment through assimilating the local observation data at these sites, the overestimation is removed with the analyzed ozone concentrations very close to the observed values. On the other hand, the forecast ozone in EXP1 is consistent with the observation except for the forecast during the first few hours. A noteworthy phenomenon is that the forecasts during the beginning 1–2 h relax a lot to the free run even with a quit good analysis. Then the departure between forecast and observation becomes smaller gradually. It indicates that the uncertainty of ozone forecast at suburban areas is reduced gradually with the continuous

ACPD
11, 7811–7849, 2011

constraint from ozone observation on its initial conditions. Generally, the surface ozone concentrations in suburban area have a relatively long life cycle and can be influenced by regional transport and vertical flux of ozone significantly. However, high-precision analyzed ozone values in three-dimensional space are not easy to be obtained within one or two hours, because there are only a few observation stations available.

Different from the previous two suburban sites, gradual improvement of ozone forecast is hardly observed at the two urban sites (Tianjin and Tangshan). An overestimation of daytime ozone at Tianjin station and an underestimation of daytime ozone at Tangshan station exist for the free run. The analysis can adjust the background ozone to the observed values quite well except for certain hours during nighttime (e.g., the first 4 h at Tangshan). However, the 1-hour forecast rapidly relaxes toward the free run especially at Tangshan station. Two things can account for the ceasing impact of ozone initial value optimization. Firstly, ozone at urban areas has a relatively short life cycle due to the rapid chemical production and destruction, which can lead to small spatial correlation scales of background field and the corresponding small influence ranges of observations. On the other hand, the errors of the freshly emitted precursors can quickly affect the short term ozone forecast at urban areas and lead to the deficiency of ozone forecast even with good ozone initial conditions. Another noteworthy phenomenon is the deficiency of EnKF in adjusting ozone initial conditions at urban sites during nighttime. It is probably due to the almost zero values of the simulated ozone concentration during nighttime, which can lead to a very small background error covariance and disregards of observation during the analysis. Further studies are needed to find out solutions for this problem.

4.2 Adjustment of precursor initial conditions

One of the goals of this study was to obtain some insights into cross-species data assimilation, with expectation to improve the accuracy of the forecast ozone concentrations. The perturbations of EnKF on the common error sources including ozone precursor initial conditions, emissions, photolysis rates and deposition velocity can

ACPD
11, 7811–7849, 2011

facilitate developing an effective cross-species data assimilation strategy. In EXP2 and EXP4, VOC initial conditions and NO_x initial conditions are adjusted, respectively, with assimilating ozone observations.

Figure 5a and b display the departure of daytime VOC in EXP2 and daytime NO in EXP4 from those in free run respectively. Significant discrepancy of VOC and NO initial concentrations can be observed in Beijing, Tianjin and Tangshan areas, where densely distributed observations are available and strong relationship between ozone and its precursor exists. It indicates that assimilating ozone observation can effectively change VOC and NO initial field. In EXP2, daytime VOC concentrations decrease in the urban areas of Beijing and Tianjin with the maximum reduction over 50 ppbv, while those in Tangshan increase. Different from the behavior of VOC, the adjustment of NO_x initial conditions with ozone observations leads to a reverse effect on NO concentrations. Increment of daytime NO concentrations in Beijing and Tianjin urban areas and reduction in Tangshan urban area are observed.

The quite different changes of VOC and NO initial conditions when ozone observations are assimilated are largely dependent on the complex nonlinear relationship between ozone and its precursors. The daytime ozone level in urban areas is mostly "VOC-limited" in Beijing and Tianjin areas, with ozone concentration positively related to VOC concentrations and negatively related to NO concentrations. Therefore, both reducing of VOC concentration and increasing of NO concentration are useful for weakening the overestimation of ozone in these areas. On the other hand, increment of VOC initial conditions or decrease of NO initial conditions would be beneficial to less the underestimation of daytime ozone in Tangshan urban area.

Figure 6 displays a comparison of the hourly RMSE of ozone forecast when the initial conditions of VOC and NO_x are adjusted separately with assimilating ozone observations. Significant improvement of ozone forecast can be observed. The daily-averaged RMSE of ozone forecast are reduced by 11% and 15% with adjusting VOC initial conditions and NO_x initial conditions respectively. It indicates that both VOC and NO_x initial conditions are good control variables of data assimilation to improve short-term ozone

ACPD
11, 7811–7849, 2011

forecast. Greater impacts of adjusting precursor initial conditions on ozone forecast occur during daytime than night time. This difference is probably related to the rapid photochemical reactions between ozone and its precursors, which only occur during daytime and make the daytime ozone level more dependent on the precursor concentrations than the nighttime ozone. On the other hand, the slightly better performance of adjusting NO_x initial conditions than adjusting VOC initial conditions during nighttime is probably due to the relatively important role of titration reaction between ozone and NO in nighttime ozone chemistry.

4.3 Adjustment of precursor emission rates

Although the relationships between ozone and its precursor emissions are nonlinear, it is still possible to describe it approximately in a linear way in the model. For example, Tang et al. (2010b) employed Monte Carlo method to identify the relationship between ozone concentrations and its precursor emissions in urban Beijing with linear regression equations. Such relationship can be used to adjust the precursor emission with observed ozone. In this study, the same random perturbation method is employed to establish the correlation between the gridded emission rate and ozone concentrations. EXP3 and EXP5 are conducted to investigate the benefits and shortcomings with adjusting the precursor emission rates when only ozone observations are used. The emission rate at each grid is taken as an independent variable. A simple localization scheme is applied to emission rate estimation: the correction of emission rates in one grid only rests on the ozone observations within 54 km distance from this grid. The adjusted emissions obtained at the analysis step are then used for the subsequent simulation. Furthermore, the correction factor is restricted to be in the range between 0.2 and 5 in order to avoid excessive furious correction and its resulting instability in model simulation.

The differences of VOC emission rates between EXP3 (experiment with adjusting VOC emission rates only) and free run during daytime are presented in Fig. 7a. The most obvious impacts of ozone data assimilation on VOC emission rates are observed

ACPD
11, 7811–7849, 2011

at the urban areas of Beijing, Tianjin and Tangshan, similar to the impact on VOC initial conditions. In the urban areas of Beijing and Tianjin, assimilating ozone observations leads to a large reduction of VOC emission rates during daytime with the maximum reduction over 50% of reference emission rates. This adjustment would be useful to compensate for the overestimation of ozone concentration in such areas. In urban areas of Tangshan, the VOC emission rates increase after the adjustment, which in turn reduces the underestimation of ozone concentrations in the model. This result indicates that assimilating ozone observations can effectively adjust VOC emission rates in urban areas with high emission rates and improve ozone forecast accordingly. In Fig. 7b, on the other hand, a reverse effect on NO_x emission rates is observed from adjusting NO_x emissions only in EXP5. This reverse effect is quite similar to that shown in the experiments for adjusting precursor initial conditions. It is noteworthy that such a revision for a single factor could not be interpreted as the optimization of the emission source as pointed out by precious studies (Hanea et al., 2004), because this revision is mainly to compensate partly for the differences between observation and simulation and reduce the root mean square error of simulation. The difference between observation and simulation in fact originates from many uncertainty sources besides emission rates. Further investigation on assessing the contribution of emission error to this difference is needed for emission inversion.

In Fig. 8a, a comparison is made between the RMSE of 1-hour ozone forecast at individual sites in EXP3 and those in free run. Similar comparison is also made in Fig. 8b for the experiment with NO_x emission adjustment. Obviously, significant improvement of ozone forecast skill at urban sites can be claimed from adjusting either VOC or NO_x emissions. The site-averaged RMSE is reduced by 19% and 38% respectively. However, almost no impact is found on ozone forecast skill at suburban sites. Local VOC and NO_x emission rates in the suburban areas are low, which may display little influence on zone concentrations compared with other factors such as regional transport. Therefore, it is quite difficult to significantly impact the ozone forecast at suburban area by correcting its relatively low emission rates. In the urban area with high emission

ACPD
11, 7811–7849, 2011

rates, precursor emissions play an important role in ozone chemistry and their uncertainties are also the key uncertainty source in ozone forecast. This results indicates that adjustment of precursor emissions would be a useful way to improve ozone forecast at urban sites. It also identifies the possibility to use ozone observations for precursor emission inversion. Of course, the complex nonlinear relationship between ozone and its precursor emissions is a great challenge for such attempt.

4.4 Simultaneous adjustment of ozone initial conditions and precursor initial conditions and emissions

The purpose of combined, simultaneous adjustment of ozone initial value, precursor initial conditions and emission rates in EXP6 is to evaluate the ability of EnKF in adjusting multi uncertainty sources with ozone observations. Figure 9 presents a comparison between the hourly RMSE of ozone forecast in EXP6 with the simultaneous adjustment strategy and those in previous experiments. It can be seen that the simultaneous adjustment outperforms the other experiments with the smallest RMSE. The daily-averaged RMSE of ozone forecast in EXP6 is 56% lower than that in free run. It indicates that the regional ozone forecast can be further improved with ozone initial conditions, precursor initial conditions and emissions adjusted simultaneously by EnKF. The simultaneous adjustment would be a valuable method to improve regional ozone forecast when only ozone observations are available. A similar result is obtained by Elbern et al. (2007), in which four-dimensional variational data assimilation method is employed to assimilate about 39 000 ozone observations a day in European and a chemical transport model with a coarse horizontal resolution of 54 km is used. On the other hand, however, there is still 11.4 ppbv of daily-averaged RMSE for 1-hour ozone forecast in EXP6. The residual errors may originate from other uncertainty sources such as vertical diffusion and dry deposition. The potentials for further improving regional ozone forecast need to be further investigated by adjusting other uncertainty sources in EnKF. Furthermore, establishing new monitoring stations for data assimilation in the regional observation network may also further improve ozone forecast.

ACPD
11, 7811–7849, 2011

In Fig. 9, the second-best forecast skill is obtained by optimizing ozone initial value. The significant improvement of forecast skill can be observed during both daytime and nighttime. The daily averaged RMSE of ozone forecast is 47% lower than that of free run, which highlights the importance of optimizing ozone initial conditions to improving short-term regional ozone forecast. On the other hand, the adjustments of two precursor initial conditions and emissions also show good performances in improving ozone forecast. However, the impacts of such adjustments are mainly reflected in improving daytime ozone forecast skill especial for adjusting VOC initial conditions and emissions. An explanation for this is the quite different characters of daytime ozone chemistry and nighttime chemistry mentioned in Sect. 3.2.

In order to evaluate the effects of the simultaneous adjustment on ozone forecast in different areas, a comparison of RMSE of 1-hour ozone forecast at individual sites in EXP6 against those in free run are made in Fig. 10. The forecast skills at both urban and suburban sites are significantly improved with the simultaneous adjustment. The RMSE of ozone forecast at urban and suburban sites are reduced by 54% and 59% respectively. Compared with EXP1 (experiment with optimizing ozone initial conditions only), further improvement of ozone forecast is clearly visible at urban sites after adjusting ozone initial value, precursor initial conditions and emission rates jointly, while it is hardly observed at suburban sites. This result is consistent with the finding from adjusting precursor initial conditions or emissions separately. It highlights the importance of adjusting precursor initial conditions and emission rates for improvement of ozone forecast at urban areas.

4.5 Sensitivity of data assimilation to ozone observations at urban and suburban sites

The regional air pollution monitoring network used in this study includes eleven urban sites and six suburban sites. An interesting issue related to the network is what different impacts of observation data at urban sites and those at suburban sites have on performance of data assimilation. To investigate this issue, we perform two data assimilation sensitivity experiments with only observations of urban sites assimilated in EXP6u and only those of suburban sites assimilated in EXP6s. The simultaneous adjustment data assimilation strategies are employed in the two experiments.

Figure 11a presents a comparison of RMSE of 1-hour ozone forecast at the urban sites in EXP0(free run), EXP6(assimilating ozone observations at all sites except for those at the three independent sites), EXP6u(assimilating ozone observations at urban sites only) and EXP6s(assimilating ozone observations at suburban sites). The RMSE of ozone forecast at urban sites in all the three data assimilation experiments are lower than that in free run. Compared with EXP6, removing observations of suburban sites mainly affects the ozone forecast in Beijing and Tianjin. Slight increases of RMSE of ozone forecast at these sites can be observed. On the other hand, removing observations of urban sites induces significant increases of RMSE of ozone forecast at all urban sites. This result indicates that ozone observations of both urban sites and suburban sites are useful for improvement of ozone forecast at urban sites. A greater role of observations at urban sites than those at suburban sites in improving ozone forecast of urban areas is shown.

A comparison of RMSE of ozone forecast at the suburban sites in the above four experiments is presented in Fig. 11b. Similar to the findings at the urban sites, the RMSE of ozone forecast at suburban sites in all the three data assimilation experiments are lower than that in free run. An interesting finding is that RMSE of ozone forecast adjusted by ozone observations of all the sites decreases by almost the same large margin as that adjusted by ozone observations of suburban sites only. Both on the other hand are smaller than the RMSE adjusted by ozone observations of urban sites only. This result exhibits the importance of the ozone observations at suburban sites on improving ozone forecast at suburban areas. Furthermore, when observed ozone data of suburban sites are assimilated, adding observations of urban sites has little impact on performance of ozone forecast at suburban sites. A most plausible reason is that the 1-hour ozone forecast of suburban sites is mainly dependent on initial

Discussion Paper | Discussion Paper | Discussion Paper | Discussion Paper |

ACPD

11, 7811–7849, 2011

Improvement of ozone forecast over Beijing

J. Zhu et al.

Title Page
Abstract Introduction
Conclusions References
Tables Figures
◂ ▸
Back Close
Full Screen / Esc
Printer-friendly Version
Interactive Discussion

ozone concentrations of its surrounding areas, which can be optimized quite well by assimilating observations of suburban sites only.

We also compared the surface field of ozone initial conditions, precursor initial conditions and emission rates in the above two sensitivity experiments against those in free run. We found that all the three factors in urban areas can be effectively adjusted through assimilating ozone observations of urban sites only. Assimilation with only suburban sites can effectively adjust ozone initial value but hardly adjust precursor initial conditions or emission rates. This result highlights the importance of urban sites for constraining the uncertainty of precursor initial conditions and emission rates.

From the previous sensitivity experiments, we can conclude that both urban sites and rural sites are important for improvement of regional ozone forecast. Further improvement of regional ozone forecast can be expected when more regional air pollution monitoring stations are established, including in suburban areas where relatively few stations are available.

5 Conclusions

In this study, ozone observational data from a newly established regional air quality monitoring network were assimilated into a high-resolution regional air quality model to improve the ozone forecast in Beijing and its surrounding areas. By using the EnKF method, we developed an assimilation strategy that can simultaneously adjust ozone initial conditions, precursor initial conditions and emissions for the modeling system. The results suggest that EnKF as a powerful tool for adjusting both state variables and emissions can bring significant improvement of regional ozone forecast. By comparing results from different data assimilation settings we investigated the separate roles of the improved ozone initial conditions, precursor initial conditions and emissions in ozone forecasting. Improving ozone initial conditions at the areas with abundant observations significantly changed the simulated ozone concentrations at the downwind areas. Improving precursor initial conditions and emissions can significantly improve

Discussion Paper | Discussion Paper | Discussion Paper | Discussion Paper |

ACPD

11, 7811–7849, 2011

the daytime ozone forecast skill at urban area although it has little effect on the ozone forecast at suburban area. It implies that precursor initial conditions and emissions are good control variables of data assimilation to improve daytime ozone forecast of urban area. Furthermore, simultaneous adjustment of ozone initial conditions and precursor initial conditions and emissions shows the best performance in improving regional ozone forecast, indicating the possibility to obtain further improvement of ozone forecast through modifying more uncertainty factors with ozone observations.

Another important finding is that ozone observations from both urban sites and suburban sites in the regional air quality monitoring network are very important for improving the regional ozone forecast, but they could have different behaviors in adjusting different control variables. This study highlights the importance of ozone observations at urban sites for constraining the uncertainty of precursor initial conditions and emission rates. Ozone observations at suburban sites are found to be quite useful for optimizing ozone initial conditions of suburban areas, which imply that they can serve as important information for improving estimation of regional ozone transport. Further improvement of regional ozone forecast can be expected when more monitoring sites are established especially at the areas with current relatively few stations.

This study provides several useful findings on how to improve the region ozone forecast at Beijing and its surrounding areas through employing the data assimilation method of EnKF. However, there are still limitations that should be stated. First of all, the uncertainty in ozone forecast comes partly from precursor initial conditions and emission rates, which is adjusted by ozone observations in this study, but the impact of the adjustment on the forecast of the two precursors VOC and NO_x has not been evaluated. Ideally a good data assimilation method should be able to optimize the modeling of the targeted variable while without degrading the modeling of other variables. Taking ozone and precursor forecast as a systematic control problem in data assimilation could obtain more insight into the uncertainty of ozone forecast, which is worthy of further investigation. Secondly, there is still more than 10 ppbv of RMSE for 1-hour ozone forecast even with the best data assimilation strategy used in this study. The

ACPD
11, 7811–7849, 2011

residual errors may originate from other uncertainty sources such as vertical diffusion and dry deposition. Further effort is needed to investigate their impacts on regional ozone forecast. Last but not least, this study focuses on the performance of different assimilation strategies on improving 1-hour ozone forecast. Longer forecast such as 24-hour or 48-hour forecast may provide opportunities to evaluate different assimilation strategies from a different time scale and enrich our understanding of their applications.

Acknowledgements. The authors would like to thank the observation group of SCAS-CERN, Institute of Atmospheric Sciences of Chinese Academy of Sciences and the observation group of College of Environmental Sciences and Engineering, Peking University for providing the observational data used for data assimilation experiments in this study. This study is funded by the 863 Key Projects (20060106A3004) and the Beijing Municipal Science and Technology Commission (D09040903670904).

References

Carmichael, G. R., Sandu, A., Chai, T. F., Daescu, D. N., Constantinescu, E. M., and Tang, Y. H.: Predicting air quality: improvements through advanced methods to integrate models and measurements, J. Computational. Physics., 227(7), 3540–3571, 2008.

Chai, T. F., Carmichael, G. R., Sandu, A., Tang, Y. H., and Daescu, D. N.: Chemical data assimilation of Transport and Chemical Evolution over the Pacific (TRACE-P) aircraft measurements, J. Geophys. Res., 111, D02301, doi:10.1029/2005JD005883, 2006.

Constantinescu, E. M., Sandu, A., Chai, T. F., and Carmichael, G. R.: Assessment of ensemble-based chemical data assimilation in an idealized setting, Atmos. Environ., 41(1), 18–36, 2007.

Elbern, H., Strunk, A., Schmidt, H., and Talagrand, O.: Emission rate and chemical state estimation by 4-dimensional variational inversion, Atmos. Chem. Phys., 7, 3749–3769, doi:10.5194/acp-7-3749-2007, 2007.

Evensen, G.: Sequential Data Assimilation with a Nonlinear Quasi-Geostrophic Model Using Monte-Carlo Methods to Forecast Error Statistics, J. Geophys. Res., 99(C5), 10143–10162, 1994.

ACPD
11, 7811–7849, 2011

Evensen, G.: The ensemble Kalman Filter: theoretical formulation and practical implementation, Ocean Dynam., 53, 343–367, 2003.
Evensen, G.: The Ensemble Kalman Filter for combined state and parameter estimation, IEEE Contr. Syst. Mag., 29(3), 83–104, 2009.
Grell, G. A., Dudhia, J., and Stauffer, D. R.: A description of the fifth-generation Penn State/NCAR mesoscale model (MM5), NCAR Technical Note, NCAR/TN-398+STR, 117 pp., 1994.
Hanea, R. G., Velders, G. J. M., and Heemink, A.: Data assimilation of ground-level ozone in Europe with a Kalman filter and chemistry transport model, J. Geophys. Res., 109, D10302, doi:10.1029/2003JD004283, 2004.
Hao, J. M., Wang, L. T., Shen, M. J., Li, L., and Hu, J. N.: Air quality impacts of power plant emissions in Beijing, Environ. Pollut., 147(2), 401–408, 2007.
Houtekamer, P. L. and Mitchell, H. L.: A sequential ensemble Kalman filter for atmospheric data assimilation, Mon. Weather Rev., 129(1), 123–137, 2001.
Houyoux, M. R., Vukovich, J. M., Coats, C. J., Wheeler, N. J. M., and Kasibhatla, P. S.: Emission inventory development and processing for the Seasonal Model for Regional Air Quality (SMRAQ) project, J. Geophys. Res., 105(D7), 9079–9090, 2000.
Li, J., Wang, Z. F., Akimoto, H., Gao, C., Pochanart, P., and Wang, X. Q.: Modeling study of ozone seasonal cycle in lower troposphere over east Asia, J. Geophys. Res., 112(D22), D22S25, doi:10.1029/2006JD008209, 2007.
Li, J., Wang, Z. F., Akimoto, H., Tang, J., and Uno, I.: Modeling of the impacts of China's anthropogenic pollutants on the surface ozone summer maximum on the northern Tibetan Plateau, Geophys. Res. Lett., 36, L24802, doi:10.1029/2009GL041123, 2009.
Li, J., Wang, Z., Wang, X., Yamaji, K., Takigawa, M., Kanaya, Y., Pochanart, P., Liu, Y., Irie, H., Hu, B., Tanimoto, H., and Akimoto, H.: Impacts of aerosols on summertime tropospheric photolysis frequencies and photochemistry over Central Eastern China, Atmos. Environ., in press, doi:10.1016/j.atmosenv.2011.01.016, 2011.
Lin, C., Wang, Z., and Zhu, J.: An Ensemble Kalman Filter for severe dust storm data assimilation over China, Atmos. Chem. Phys., 8, 2975–2983, doi:10.5194/acp-8-2975-2008, 2008a.
Lin, C., Zhu, J., and Wang, Z.: Model bias correction for dust storm forecast using ensemble Kalman filter, J. Geophys. Res., 113, D14306, doi:10.1029/2007JD009498, 2008b.
Shao, M., Tang, X. Y., Zhang, Y. H., and Li, W. J.: City clusters in China: air and surface water

ACPD
11, 7811–7849, 2011

pollution, Front. Ecol. Environ., 4, 353–361, 2006.
Streets, D. G., Fu, J .H. S., Jang, C. J., Hao, J. M., He, K. B., Tang, X. Y., Zhang, Y. H., Wang, Z. F., Li, Z. P., Zhang, Q., Wang, L. T., Wang, B. Y., and Yu, C.: Air quality during the 2008 Beijing Olympic Games, Atmos. Environ., 41(3), 480–492, 2007.
Sudo, K. M., Takahashi, J., Kurokawa, and Akimoto, H.: CHASER: A global chemical model of the troposphere 1.Model description, J. Geophys. Res., 107(D17), 4339, doi:10.1029/2001JD001113, 2002.
Tang, X., Wang, Z. F., Zhu, J., Wu, Q. Z., and Gbaguidi, A.: Ensemble-based surface ozone forecast over Beijing, Climate and Environmental Research, 15(5), 677–684, 2010a (in Chinese).
Tang, X., Wang, Z. F., Zhu, J., Wu, Q. Z., and Gbaguidi, A.: Preliminary application of Monte Carlo uncertainty analysis in ozone simulation, Climate and Environmental Research, 15(5), 541–550, 2010b (in Chinese) .
Tang, X., Wang, Z. F., Zhu, J., Gbaguidi, A., Wu, Q. Z., Li, J., and Zhu, T.: Sensitivity of ozone to precursor emissions in urban Beijing with a Monte Carlo scheme, Atmos. Environ., 44, 3833–3842, 2010c.
van Loon, M., Builtjes, P. J. H., and Segers, A. J.: Data assimilation of ozone in the atmospheric transport chemistry model LOTOS, Environ. Model. Softw., 15, 603–609, 2000.
Wang, Z., Akimoto, H., and Uno, I.: Neutralization of soil aerosol and its impact on the distribution of acid rain over East Asia: Observations and model results, J. Geophys. Res., 107(D19), 4389, doi:10.1029/2001JD001040, 2002.
Wang, Z., Li, J., Wang, X., Pochanart, P., and Akimoto, H.: Modeling of regional high ozone episode observed at two mountain sites (Mt. Tai and Huang) in East China, J. Atmos. Chem., 55(3), 253–272, doi:10.1007/s10874-006-9038-6, 2006a.
Wang, Z. F., Xie, F. Y., Wang, X. Q., An, J. L., and Zhu, J.: Development and application of Nested Air Quality Prediction Modeling System, Chinese J. Atmos. Sci., 30, 778–790, 2006b (in Chinese).
Wang, Y., Hao, J., McElroy, M. B., Munger, J. W., Ma, H., Chen, D., and Nielsen, C. P.: Ozone air quality during the 2008 Beijing Olympics: effectiveness of emission restrictions, Atmos. Chem. Phys., 9, 5237–5251, doi:10.5194/acp-9-5237-2009, 2009.
Wesely, M. L.: Parameterization of surface resistances to gaseous dry deposition in regional-scale numerical models, Atmos. Environ., 23, 1293–1304, 1989.
Wu, L., Mallet, V., Bocquet, M., and Sportisse, B.: A comparison study of data

ACPD
11, 7811–7849, 2011

Improvement of ozone forecast over Beijing

J. Zhu et al.

assimilation algorithms for ozone forecasts, J. Geophys. Res., 113(D20), D20310, doi:10.1029/2008JD009991, 2008.

Wu, Q. Z., Wang, Z. F., Gbaguidi, A., Gao, C., Li, L. N., and Wang, W.: A numerical study of the contribution to the air pollutant in Beijing during CAREBeijing-2006, Atmos. Chem. Phys. Discuss., 11, 5271–5312, doi:10.5194/acpd-11-5271-2011, 2011.

Xin, J. Y., Wang, Y. S., Tang, G. Q., Wang, L. L., Sun, Y., Wang, Y. H., Hu, B., Song, T., Ji, D. S., Wang, W. F., Li, L., and Liu, G. R.: Variability and reduction of atmospheric pollutants in Beijing and its surrounding area during the Beijing 2008 Olympic Games, Chinese Sci. Bull., 55(18), 1937–1944, 2010 (in Chinese).

Zaveri, R. A. and Peters, L. K.: A new lumped structure photochemical mechanism for large-scale applications, J. Geophys. Res., 104(D23), 30387–30415, 1999.

Zhang, Q., Streets, D. G., Carmichael, G. R., He, K. B., Huo, H., Kannari, A., Klimont, Z., Park, I. S., Reddy, S., Fu, J. S., Chen, D., Duan, L., Lei, Y., Wang, L. T., and Yao, Z. L.: Asian emissions in 2006 for the NASA INTEX-B mission, Atmos. Chem. Phys., 9, 5131–5153, doi:10.5194/acp-9-5131-2009, 2009.

Zhu., J., Lin, C., and Wang, Z.: Dust storm ensemble forecast experiments in East Asia, Adv. in Atmos. Sci., 26(6), 1053–1070, 2009.

Zou, Y. F., Wu, Q., Wang, Z. F., and Zhu, J.: Update of industrial pollution source in Hebei and its effects on regional air quality modeling during 2008 Beijing Olympics Games, Climate and Environmental Research, 15(5), 624–635, 2010(in Chinese).

ACPD

11, 7811–7849, 2011

Table 1. Experiments designed for evaluating the performance of different data assimilation strategies.

Experiments	Control variables defined in EnKF					Ozone observations assimilated	Ozone observations for forecast evaluation
	O_3 initial conditions	VOC initial conditions	VOC emission rates	NO_x initial conditions	NO_x emission rates		
EXP0	×	×	×	×	×	None	All sites
EXP1	√					nine urban sites five suburban sites	All sites
EXP2		√				the same sites as EXP1	All sites
EXP3			√			the same sites as EXP1	All sites
EXP4				√		the same sites as EXP1	All sites
EXP5					√	the same sites as EXP1	All sites
EXP6	√	√	√	√	√	the same sites as EXP1	All sites
EXP6u	√	√	√	√	√	the same nine urban sites as EXP1	All sites
EXP6s	√	√	√	√	√	the same five suburban sites as EXP1	All sites

ACPD
11, 7811–7849, 2011

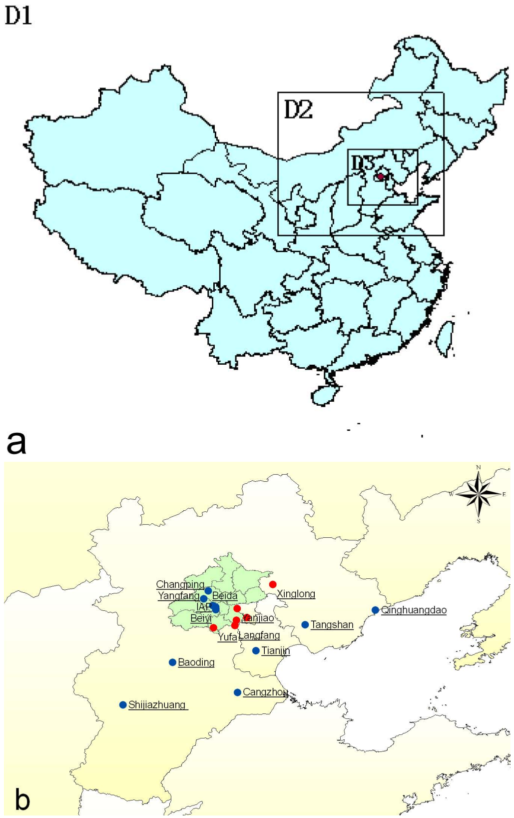

Fig. 1. (a) Model domains. The first domain covers East Asia with 81 km × 81 km resolution; the second domain consists of North China with 27 km × 27 km resolution; the third domain includes Beijing and its surrounding areas with 9 km × 9 km resolution. **(b)** Monitoring stations. The six suburban stations are marked as red dots and the eleven urban stations are represented by blue dots.

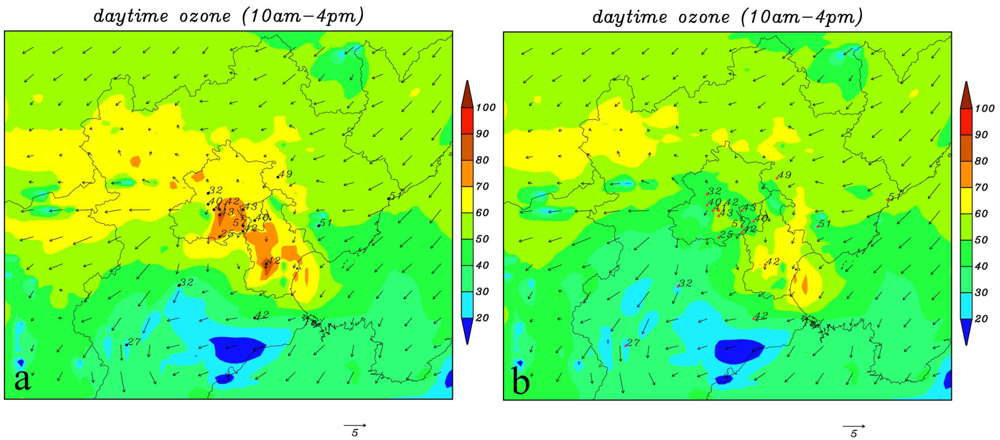

Fig. 2. Simulated daytime ozone concentrations (ppbv) in the third domain obtained from **(a)** free run and **(b)** EXP1 with ozone initial conditions optimized. The observed daytime ozone values (numbers near red dots) at monitoring stations are also shown.

ACPD
11, 7811–7849, 2011

Improvement of ozone forecast over Beijing

J. Zhu et al.

Title Page
Abstract Introduction
Conclusions References
Tables Figures
◀| |▶
◀ ▶
Back Close
Full Screen / Esc
Printer-friendly Version
Interactive Discussion

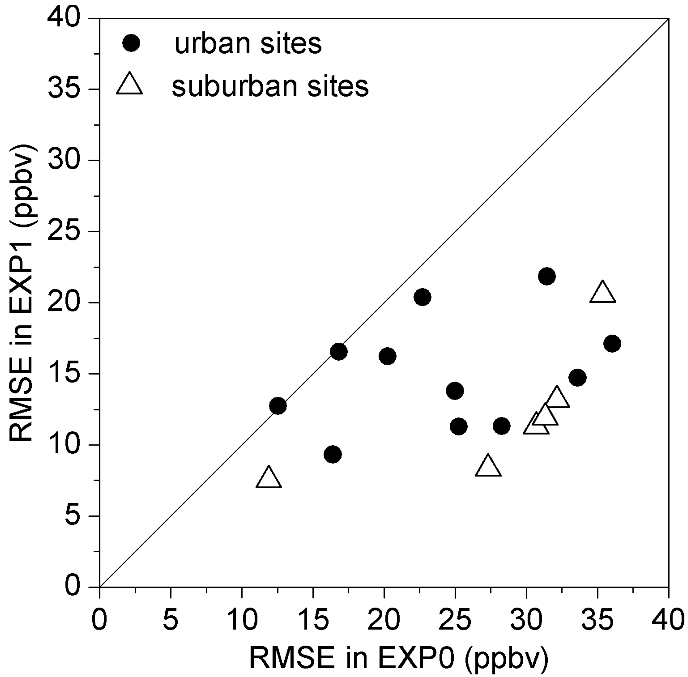

Fig. 3. Comparison of RMSE of 1-hour ozone forecast at urban sites (dots) and suburban sites (triangles) in free run against those in EXP1.

ACPD
11, 7811–7849, 2011

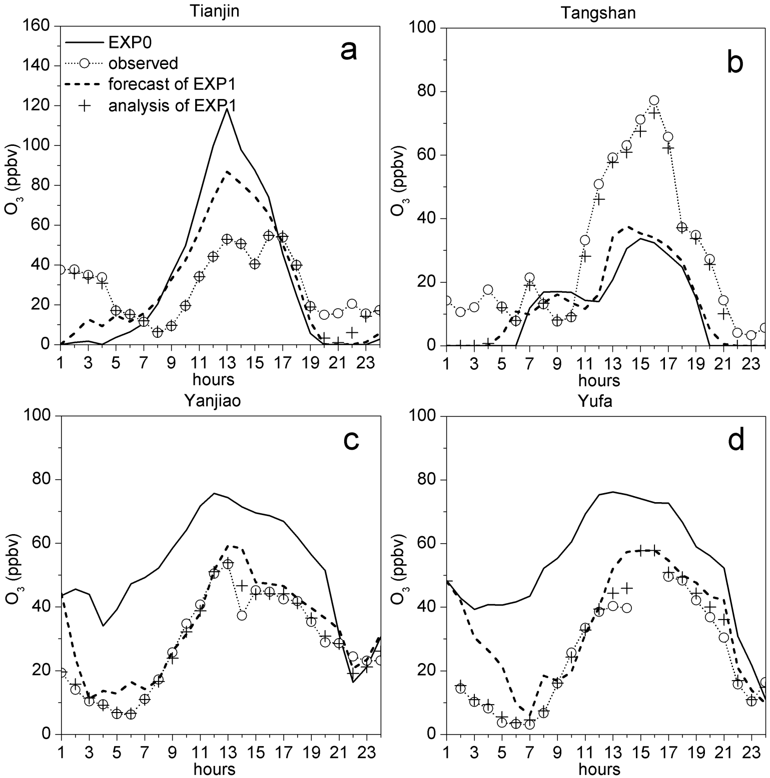

Fig. 4. Time series of the hourly ozone concentrations obtained from observation (dash line with circles), free run (solid line), analysis (plus signs) and 1-hour forecast in EXP1 (dash line) at two urban sites (Tianjin and Tangshan) and at two suburban sites (Yanjiao and Yufa).

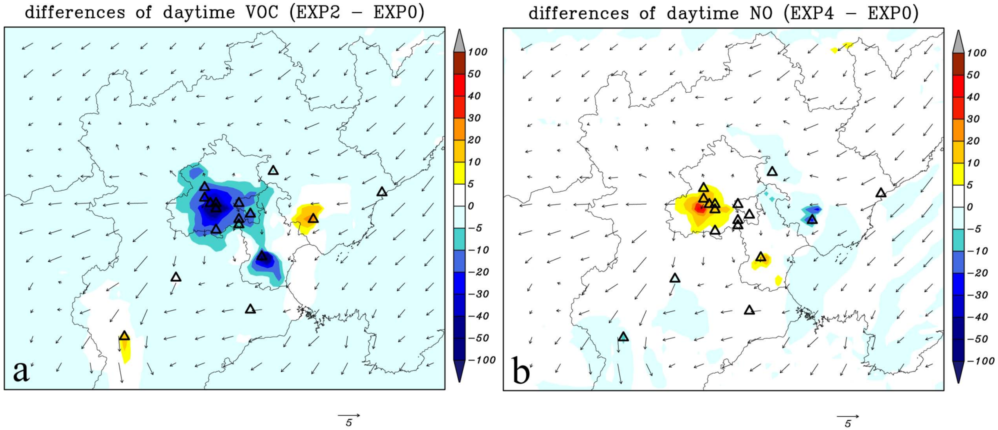

Fig. 5. (a) Departure of daytime VOC concentrations (ppbv) in EXP2 (experiment with adjusting VOC initial conditions only) from those in free run between 10:00 a.m. to 04:00 p.m. on 13 August 2008 (LT); **(b)** Departure of daytime NO concentrations (ppbv) in EXP4 (experiment with adjusting NO_x initial conditions only) from those in free run 10:00 a.m. to 04:00 p.m. on 13 August 2008 (LT).

ACPD
11, 7811–7849, 2011

Improvement of ozone forecast over Beijing

J. Zhu et al.

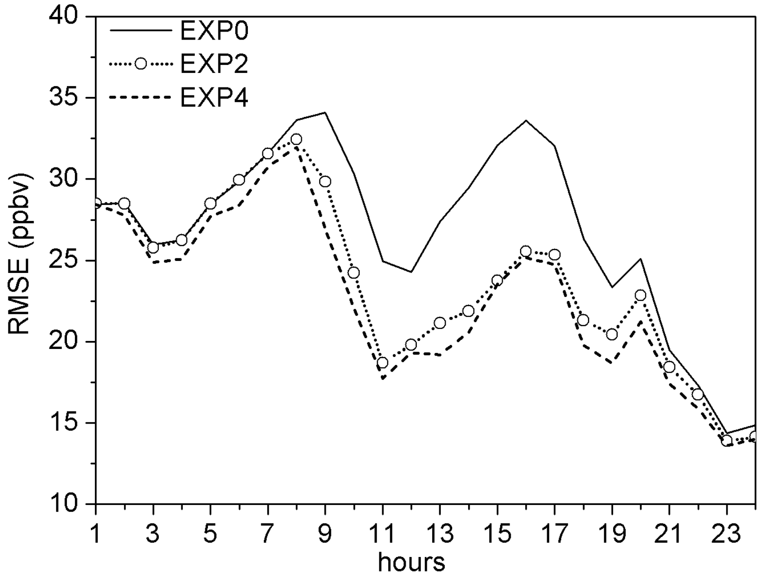

Fig. 6. Time series of hourly RMSE of 1-hour ozone forecast in free run (solid line), EXP2 (dash line with circles) and EXP4 (dash line).

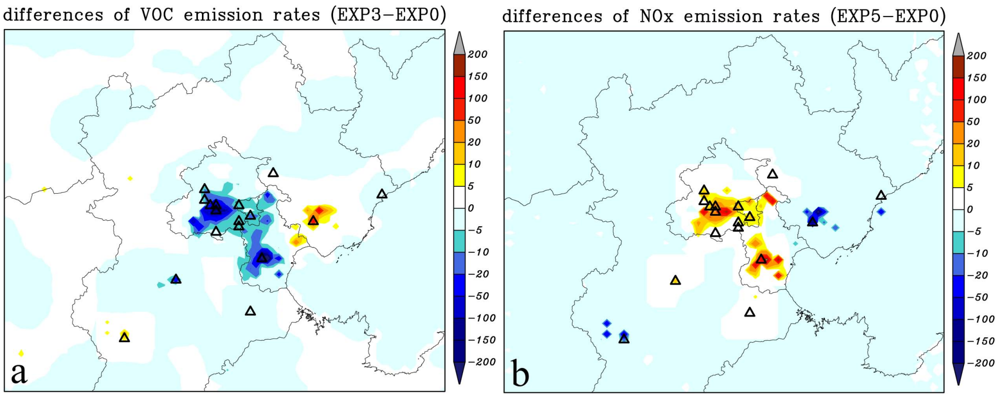

Fig. 7. (a) Departure of VOC emission rates (ton/km^2 year^{-1}) in EXP3 (experiment with adjusting VOC emission rates only) from those in free run between 10:00 a.m. to 04:00 p.m. on 13 August 2008 (LT); **(b)** Departure of NO_x emission rates (ton/km^2 year^{-1}) in EXP5 (experiment with adjusting NO_x emission rates only) from those in free run between 10:00 a.m. to 04:00 p.m. on 13 August 2008 (LT).

ACPD
11, 7811–7849, 2011

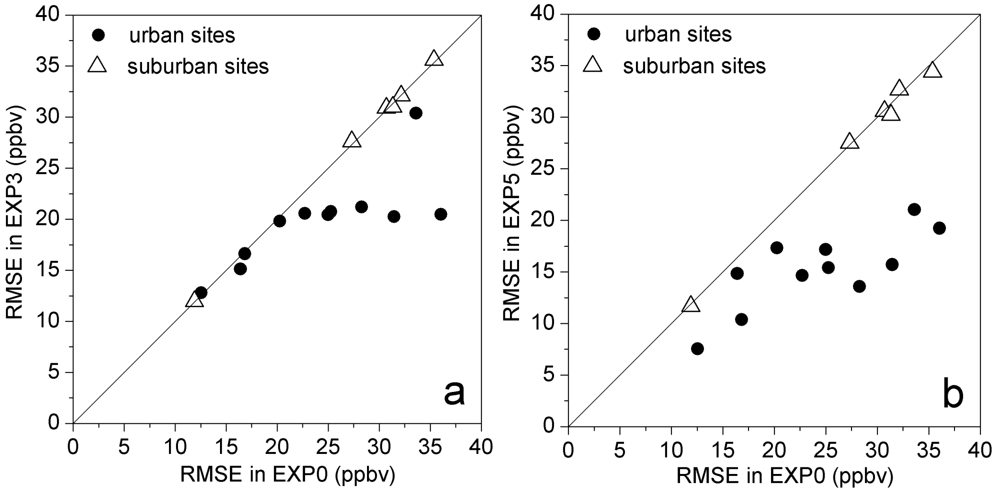

Fig. 8. (a) RMSE of 1-hour ozone forecast at urban sites (dots) and suburban sites (triangles) in free run against those in EXP3 and **(b)** against those in EXP5.

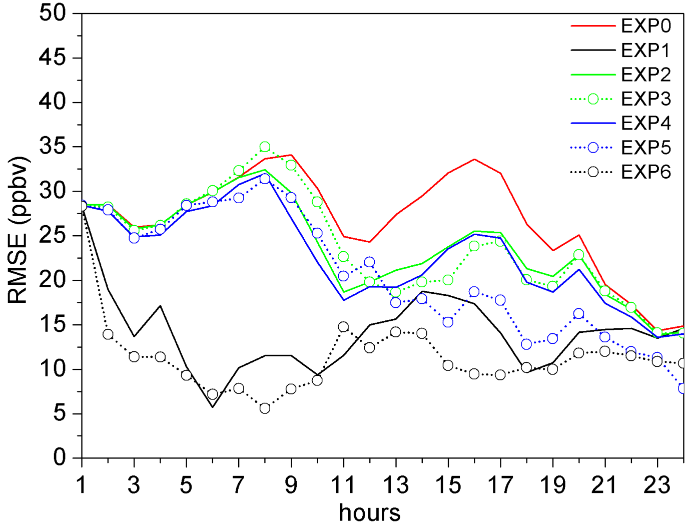

Fig. 9. Hourly RMSE of 1-hour ozone forecast in EXP0 (free run), EXP1 (optimizing ozone initial conditions only), EXP2 (adjusting VOC initial conditions only), EXP3 (adjusting VOC emission rates only), EXP4 (adjusting NO_x initial conditions only), EXP5 (adjusting VOC emission rates only) and EXP6 (adjusting ozone initial conditions and precursor NO_x, VOC initial conditions and emission rates jointly).

ACPD
11, 7811–7849, 2011

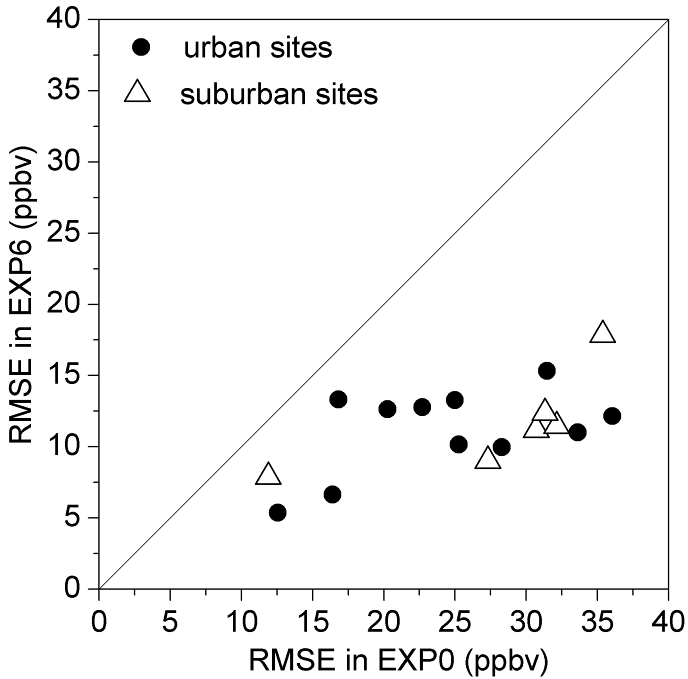

Fig. 10. Comparison of RMSE of 1-hour ozone forecast at urban sites (dots) and suburban sites (triangles) in free run against those in EXP6.

ACPD
11, 7811–7849, 2011

Improvement of ozone forecast over Beijing

J. Zhu et al.

Title Page
Abstract Introduction
Conclusions References
Tables Figures
Back Close
Full Screen / Esc
Printer-friendly Version
Interactive Discussion

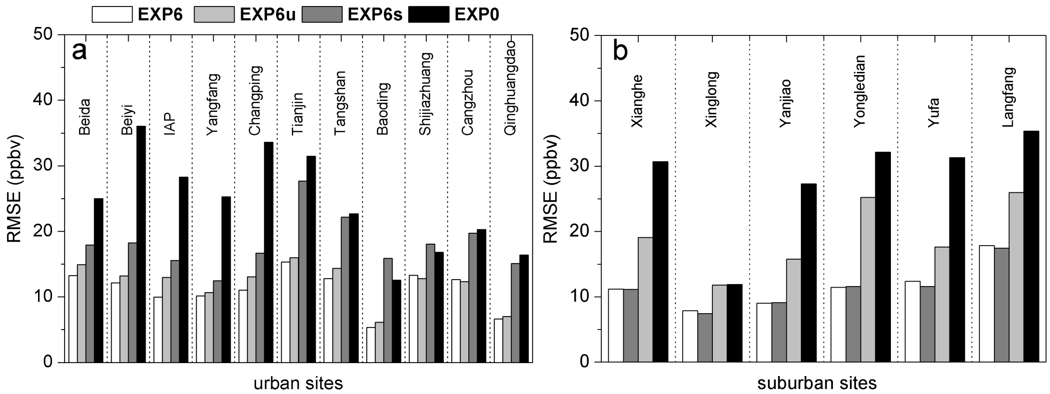

Fig. 11. Comparison of RMSE in free run, EXP6 (with ozone observations at all sites except for three independent sites assimilated), EXP6u (with ozone observations at nine urban sites assimilated) and EXP6s (with ozone observations at five suburban sites assimilated) for **(a)** the 1-hour ozone forecast at eleven urban sites and **(b)** the 1-hour ozone forecast at six suburban sites.

ACPD
11, 7811–7849, 2011